
Test-Time Adaptation for Non-stationary Time Series: From Synthetic Regime Shifts to Financial Markets

Yurui Wu, Qingying Deng, Wonou Chung, Mairui Li

Department of Statistics & Operations Research, UNC Chapel Hill
Chapel Hill, NC, 27599

{yuruiwu,doradeng,wchung,mairuili}@email.unc.edu

Abstract

Time series encountered in practice are rarely stationary. When the data distribution changes, a forecasting model trained on past observations can lose accuracy. We study a small-footprint test-time adaptation (TTA) framework for causal time-series forecasting and direction classification. The backbone is frozen, and only normalization affine parameters are updated using recent unlabeled windows. For classification we minimize entropy and enforce temporal consistency; for regression we minimize prediction variance across weak time-preserving augmentations and optionally distill from an EMA teacher. A quadratic drift penalty and an uncertainty-triggered fallback keep updates stable. We evaluate this framework in two stages: synthetic regime shifts on ETT benchmarks, and daily equity and FX series (SPY, QQQ, EUR/USD) across pandemic, high-inflation, and recovery regimes. On synthetic gradual drift, normalization-based TTA improves forecasting error, while in financial markets a simple batch-normalization statistics update is a robust default and more aggressive norm-only adaptation can even hurt. Our results provide practical guidance for deploying TTA on non-stationary time series. The source code of this study is available at this [Google Drive](#).

1 Introduction

Real-world time series, such as financial prices or electricity loads, evolve over time. Structural breaks, policy changes, and macroeconomic shocks can shift both the level and the volatility of the process. During the COVID-19 crisis and the subsequent high-inflation period, market dynamics changed rapidly, and models trained on pre-crisis data became miscalibrated. Once the deployment distribution departs from the training distribution, minimizing training loss is no longer sufficient to guarantee test performance.

Test-time adaptation (TTA) addresses this issue by updating part of the model using unlabeled test inputs. For time series, a practical TTA scheme must be causal (no future data), parameter efficient, and robust to noisy updates. In this work we freeze the backbone and adapt only a small parameter set at deployment. When day t arrives, we collect the most recent windows, apply weak time-preserving augmentations, and take a few gradient steps on unsupervised objectives. For classification we combine entropy minimization with temporal consistency; for regression we minimize augmentation variance and optionally distill from an exponential-moving-average teacher. We control the size of daily parameter changes and fall back to a lightweight batch-normalization statistics update when an uncertainty proxy is high.

Our goal is not to propose a new heavy architecture, but to understand when small-footprint TTA helps or hurts on non-stationary sequences. We make three contributions. First, we unify several TTA choices—no adaptation, batch-normalization statistics refresh, and norm-only adaptation—under one causal framework. Second, we evaluate this framework in two stages: synthetic shifts on ETT

benchmarks, and real markets (SPY, QQQ, EUR/USD) split into pandemic, high-inflation, and recovery regimes. Third, we connect the results with econometric tools (Diebold–Mariano tests and Newey–West adjustments) and summarize practical recommendations for deploying TTA in streaming forecasting systems.

2 Literature Review

2.1 Test-time adaptation under distribution shift

TTA minimizes an unsupervised objective at inference using the current test inputs, while most parameters are frozen. A central result is that tuning only normalization affine parameters (γ, β) by entropy minimization can yield large gains under covariate shift [1]. This works because normalization re-centers and re-scales hidden activations to match the present input distribution, and the affine degrees of freedom are enough to correct many first/second-moment changes. In streaming scenarios, adaptation can accumulate error if the procedure is aggressive or if pseudo-targets are unstable. Prior work proposes stabilizers such as exponential-moving-average teachers and conservative update schedules [2, 3]. We follow this line by using an EMA teacher for self-distillation in regression and by adding a quadratic drift penalty that discourages large inter-day parameter motion.

Refreshing batch-normalization statistics at test time (recomputing means and variances without gradients) already improves robustness to small-batch and covariate shifts [4, 5]. This motivates our fallback: when an uncertainty proxy is high, we refresh statistics and skip gradient updates. Recent analyses add explanatory depth; for example, Kim and Lee et al. [21] show that TTA can increase linearity in intermediate layers, which yields more stable extrapolation on shifted inputs. For forecasting, test-time learning can be formulated with variance and consistency objectives that do not require labels [22]. Adaptation in non-stationary environments can also be framed as representation alignment that maintains proximity between current and reference features [20]. Our consistency and variance objectives, together with EMA-teacher and drift control, are concrete realizations of these ideas for time series.

2.2 Normalization and architectures for non-stationary sequences

Non-stationarity often manifests as level/scale drift and time-varying seasonality, so normalization layers are a primary tool. Reversible instance normalization (RevIN) standardizes each sequence and then reverses the transform before output; it reduces train–test mismatch while preserving the forecasting target [6]. Adaptive normalization learns gates that respond to distributional changes [7]. Frequency-aware normalization emphasizes multi-scale periodic structure and modulates features accordingly [8]. These methods act within the backbone. Our TTA instead acts on top of such defenses, allowing small affine corrections that follow the deployment stream, so the two approaches are complementary. On the architecture side, the Non-Stationary Transformer incorporates evolving statistics directly into attention and residual paths [9]. For our hosts we adopt light yet competitive models—multi-scale residual Temporal Convolutional Networks (TCN) [10] and compact Transformers—as well as PatchTST and TimesNet as references [11, 12]. We select small widths (64–128) and few layers (2–4) to ensure that test-time updates touch only thousands of parameters, keeping latency negligible while preserving accuracy.

2.3 Regime-wise evaluation and econometric significance

Statistical performance should be interpreted by regime. Markov-switching models explain how coefficients and volatility change across states [14], and survey evidence supports regime-dependent predictability in financial markets [15]. We therefore report rolling curves and regime-wise summaries. To compare forecast accuracy we use the Diebold–Mariano test with HAC variance estimation [16, 17]. When we evaluate many variants, standard multiple-comparison corrections may be anti-conservative; Reality Check and SPA address data-snooping by bootstrapping the maximum performance statistic across models [18, 19]. Our significance reporting is aligned with these tools.

3 Problem Setup

Let $\{x_t\}_{t=1}^T$, $x_t \in \mathbb{R}^d$ be a multivariate series. We form an input window $X_t = [x_{t-L+1}, \dots, x_t] \in \mathbb{R}^{L \times d}$ and study two tasks.

1. Classification: predict the direction for day $t+1$; let $y_{t+1} \in \{0, 1\}$ denote down or up, and let $\hat{p}(X_t) \in [0, 1]^2$ be the predicted probability. We track accuracy, F1, AUC, direction accuracy, and expected calibration error (ECE), and draw reliability diagrams.
2. Regression: predict next-day log-return $r_{t+1} = \log p_{t+1} - \log p_t$ or H -day cumulative log-return $r_{t+1:t+H} = \sum_{h=1}^H r_{t+h}$; we report MAE, RMSE, and R^2 .

The deployment stream $\{P_t\}$ is non-stationary relative to training P_{train} , with shifts including location-scale drift, noise inflation, and structural changes. Synthetic generators in Appendix B implement these. For daily equity and FX series we use a unified split: train 2000–2016, validation 2017–2019, test 2020–2025. All scalers are fit on training only, and we avoid exogenous variables to prevent leakage. ETT benchmarks follow their standard splits.

4 Method

We train a backbone f_θ on the training split with supervised losses. At test time we adapt a small parameter set on unlabeled windows from the current stream; the backbone is frozen.

4.1 Backbones and updateable units

We consider a multi-scale residual TCN and a compact Transformer (2–4 layers, width 64–128). GRU/LSTM serve as references. At test time, we compare the following options:

- **no_tta**: no test-time adaptation, frozen model.
- **bn_stats**: refresh batch-normalization (BN) means and variances using the current batch, no gradients.
- **norm_only**: update only normalization affine parameters (γ, β) .

4.2 Unsupervised objectives

Let \mathcal{B} be the batch of recent unlabeled windows. For classification we use entropy and consistency:

$$\mathcal{L}_{\text{ent}}(\theta) = \frac{1}{|\mathcal{B}|} \sum_{X \in \mathcal{B}} \left(- \sum_c \hat{p}_c(X) \log \hat{p}_c(X) \right), \quad (1)$$

$$\mathcal{L}_{\text{cons}}(\theta) = \frac{1}{|\mathcal{B}|} \sum_{X \in \mathcal{B}} \|\hat{p}(X) - \hat{p}(T(X))\|_2^2, \quad (2)$$

where T is a weak time-preserving transform (Section 4.4). For regression we use variance minimization and EMA-teacher self-distillation:

$$\mathcal{L}_{\text{var}}(\theta) = \frac{1}{|\mathcal{B}|} \sum_{X \in \mathcal{B}} \text{Var}(\{\hat{y}(T_k(X))\}_{k=1}^K), \quad (3)$$

$$\mathcal{L}_{\text{sd}}(\theta, \tilde{\theta}) = \frac{1}{|\mathcal{B}|} \sum_{X \in \mathcal{B}} \|\hat{y}(X) - \tilde{y}(X)\|_2^2, \quad \tilde{\theta} \leftarrow \rho \tilde{\theta} + (1 - \rho) \theta. \quad (4)$$

Drift control: we penalize inter-day change in the small parameter set,

$$\mathcal{L}_{\text{drift}}(\theta^{(t)}, \theta^{(t-1)}) = \gamma \|\theta^{(t)} - \theta^{(t-1)}\|_2^2. \quad (5)$$

Total objective: for classification,

$$\mathcal{L}(\theta) = \alpha \mathcal{L}_{\text{ent}} + \beta \mathcal{L}_{\text{cons}} + \mathcal{L}_{\text{drift}}, \quad (6)$$

and for regression,

$$\mathcal{L}(\theta) = \alpha \mathcal{L}_{\text{var}} + \beta \mathcal{L}_{\text{sd}} + \mathcal{L}_{\text{drift}}. \quad (7)$$

Appendix A provides derivations and gradients for norm-only parameters, including proximal interpretations of the drift penalty and the variance-reduction role of the EMA teacher.

4.3 Uncertainty-triggered fallback

We compute an uncertainty proxy on \mathcal{B} . For classification, we use mean entropy $u_t = \frac{1}{|\mathcal{B}|} \sum_X H(\hat{p}(X))$. For regression, we use mean augmentation variance $u_t = \frac{1}{|\mathcal{B}|} \sum_X \text{Var}(\{\hat{y}(T_k(X))\}_k)$. We set τ as the 80th percentile of u_t on validation; 70% and 90% are ablated. If $u_t > \tau$, we refresh BN statistics and skip gradient updates.

4.4 Causality-preserving augmentations

We use weak transforms that keep time order and avoid leakage: amplitude scaling ($1 \pm 5\%$), Gaussian jitter with standard deviation 0.01 times the training standard deviation, time jitter by ± 1 step within the window, and time cutout masking up to 5 steps.

4.5 Daily test-time adaptation algorithm

Default hyperparameters are $W=64$, $S=5$, learning rate 10^{-4} , and $\alpha = \beta = 1$, $\gamma = 10^{-3}$.

Algorithm 1: Causal Test-Time Adaptation for Day t

Input: Frozen backbone f_θ ; updatable parameter set $\phi \subset \theta$ (norm-only BN affine parameters); Window length L ; context size W ; steps S ; learning rate η ; uncertainty threshold τ ; Loss type: classification ((6)) or regression ((7)); transforms $\{T_k\}$.
Output: Prediction \hat{y}_{t+1} (or \hat{p}_{t+1}) for the next day.

```

1 Build unlabeled batch  $\mathcal{B} \leftarrow \{X_{t-W+1}, \dots, X_t\}$ .
2 Compute uncertainty  $u_t$  (entropy or augmentation variance).
3 if  $u_t > \tau$  then
4   Refresh BN running statistics on  $\mathcal{B}$ ; return  $\hat{y}_{t+1} \leftarrow f_\theta(X_t)$ .
5 for  $s = 1$  to  $S$  do
6   if classification then
7     Sample a weak transform  $T$ ; compute  $\mathcal{L}_{\text{ent}}$  and  $\mathcal{L}_{\text{cons}}$ .
8      $\mathcal{L} \leftarrow \alpha \mathcal{L}_{\text{ent}} + \beta \mathcal{L}_{\text{cons}} + \gamma \|\phi - \phi^{\text{prev}}\|_2^2$ .
9   else
10    regression
11    Sample  $K$  transforms  $\{T_k\}$ ; compute  $\mathcal{L}_{\text{var}}$  and optionally  $\mathcal{L}_{\text{sd}}$ .
12     $\mathcal{L} \leftarrow \alpha \mathcal{L}_{\text{var}} + \beta \mathcal{L}_{\text{sd}} + \gamma \|\phi - \phi^{\text{prev}}\|_2^2$ .
13    Update only  $\phi \leftarrow \phi - \eta \nabla_\phi \mathcal{L}$  (SGD/Adam).
14 return  $\hat{y}_{t+1} \leftarrow f_\theta(X_t)$  with updated  $\phi$ .

```

4.6 Ablations and sensitivity

Only thousands of parameters are updated, so extra latency per test day is small on a single T4 GPU. For the hyperparameters, we sweep $W \in \{32, 64, 96\}$, $S \in \{1, 3, 5\}$, and learning rate in $\{5 \times 10^{-5}, 10^{-4}, 2 \times 10^{-4}\}$. We compare entropy-only vs. consistency-only vs. combined for classification, and variance-only vs. variance plus EMA teacher for regression. We examine augmentation sets: scaling only; scaling plus jitter; scaling plus jitter and cutout.

5 Data and Shift Construction

Stage I: ETT with synthetic shifts. We use ETTh1/ETTh2 (hourly) and ETTm1/ETTm2 (15-min). These series include power transformer loads and temperatures with clear seasonality. We generate three synthetic shifts: (i) gradual mean/variance drift, (ii) local noise inflation, and (iii) structural switches in periodic components. Formal definitions and grids are in Appendix B.

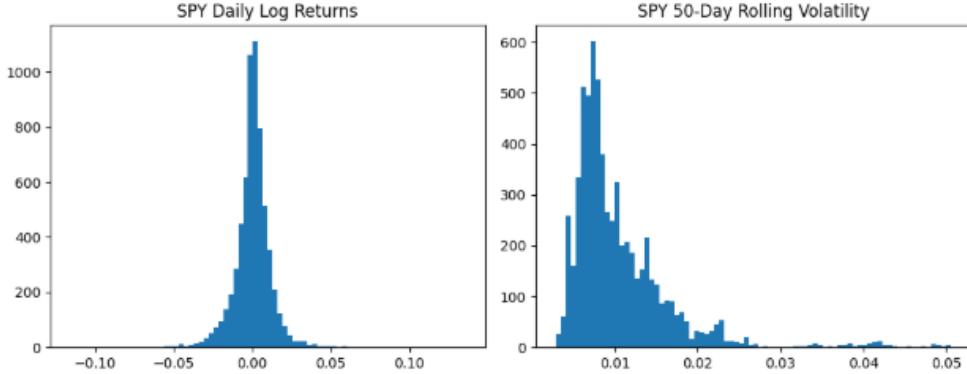


Figure 1: Regime diagnostics for SPY volatility and returns.

Stage II: equity and FX markets. We use daily SPY and QQQ index ETFs, plus EUR/USD exchange rates. Features are built from OHLCV only and standardized using training statistics:

$$\begin{aligned}
r_t &= \log(C_t) - \log(C_{t-1}), \\
\text{MOM}_t^{(N)} &= \log(C_t) - \log(C_{t-N}), \\
\text{REV}_t^{(N)} &= - \sum_{i=1}^N r_{t-i}, \\
\text{ATR}_t &= \text{EMA}(\max\{H_t - L_t, |H_t - C_{t-1}|, |L_t - C_{t-1}|\}), \\
\sigma_{P,t}^2 &= \frac{1}{4 \ln 2} (\log(H_t/L_t))^2, \quad \sigma_{GK,t}^2 = \frac{1}{2} (\log(H_t/L_t))^2 - (2 \ln 2 - 1) (\log(C_t/O_t))^2.
\end{aligned}$$

We split testing into three regimes: (1) pandemic (2020), (2) high-inflation (2021–2023), (3) recovery (2024–2025). Figure 1 shows basic regime diagnostics for SPY.

6 Experimental Protocol

We evaluate our test-time adaptation framework on three financial direction classification tasks (SPY, QQQ, and EUR/USD) and one long-horizon time-series forecasting task (ETTh1). All datasets are preprocessed into fixed-length sliding windows with input length $L = 96$, and ETTh1 is evaluated with forecast horizon $H = 96$. Data are split chronologically into training, validation, and test sets to ensure strict out-of-sample evaluation. All models use a Temporal Convolutional Network (TCN) with three residual blocks, hidden dimension 64, and kernel size 3, followed by a linear head for either classification or regression.

Models are trained using AdamW with learning rate 10^{-4} , batch size 512, and early stopping based on validation AUC (classification) or validation MSE (regression). At deployment, three main modes are compared: no adaptation (no_tta), batch-normalization statistics refresh (bn_stats), and norm-only parameter adaptation (norm_only). Test-time adaptation is triggered using an uncertainty threshold τ estimated as the 0.8 quantile of validation uncertainty, computed via prediction entropy for classification and variance of stochastic augmentations for regression. When triggered, norm-only parameters are updated using a small number of unsupervised gradient steps with entropy/consistency loss for classification or variance/distillation loss for regression. Evaluation is performed strictly on the test set using accuracy, F1, AUC, and ECE for classification; MAE, RMSE, and R^2 for regression; along with rolling performance, reliability diagrams, Diebold–Mariano statistical tests, and a simple directional trading backtest with Newey–West adjusted statistics.

Table 1: Representative ETTh1 results under synthetic regime shifts. Each entry corresponds to one representative configuration in the specified regime.

Method	Shift	MAE	RMSE	R^2
no_tta	Gradual	0.22	0.28	-0.31
norm_only	Noise	0.29	0.35	-0.02
bn_stats	Structural	1.26	1.62	-20.80

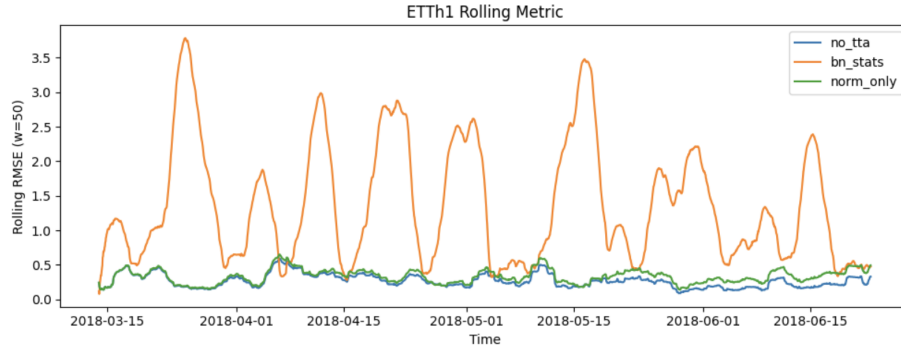


Figure 2: Rolling forecast metrics on ETTh1 under gradual drift.

7 Results

7.1 Stage I: synthetic shifts on ETT

We first study how different TTA choices behave under controlled shifts on ETTh1. Table 1 reports mean absolute error (MAE), root mean squared error (RMSE), and R^2 for one representative configuration in each synthetic regime: gradual drift, local noise inflation, and structural switches. Negative R^2 values indicate that the model performs worse than a simple training-baseline benchmark under the corresponding shift.

Norm-only adaptation is most effective under gradual mean/variance drift, where updating normalization affine parameters can track slow changes in scale and level. Under local noise inflation, variance minimization across weak augmentations stabilizes regression outputs and reduces the impact of noise bursts. Structural switches are the hardest case: even with bn_stats, errors remain large and R^2 is strongly negative.

Figure 2 shows rolling forecast metrics on ETTh1 under gradual drift. Compared with the frozen baseline, norm-only TTA reduces errors in the later part of the horizon, where the synthetic drift accumulates. This supports the view that normalization-based updates are well suited to smooth low-order moment shifts.

7.2 Stage II: equity and FX markets

We next evaluate direction classification on SPY, QQQ, and EUR/USD with the same TTA recipe. Table 2 reports cross-market direction accuracy for all three methods. The baseline accuracy is close to 0.5 on all series, reflecting the difficulty of daily direction prediction.

These numbers come from a run focused on directional accuracy; absolute values differ from other experiments, but patterns are consistent. There is no single winner: different markets and regimes prefer different TTA variants. On SPY, norm_only achieves the best directional accuracy, slightly ahead of no_tta and bn_stats. On QQQ, bn_stats provides the largest gain, while norm_only can hurt performance. On EUR/USD, both TTA methods are roughly on par with or slightly better than the frozen baseline.

Figure 3 plots rolling direction accuracy and RMSE for SPY, QQQ, and EUR/USD with regime shading. For SPY, improvements from TTA are concentrated in the pandemic and early recovery periods, when distributional change is strong. For QQQ, batch-normalization statistics updates

Table 2: Directional accuracy on test sets (2020–2025) for equity and FX markets.

Method	SPY	QQQ	EURUSD	Avg. rank
no_tta	0.504	0.503	0.516	2.33
bn_stats	0.498	0.525	0.520	1.66
norm_only	0.512	0.463	0.516	2.00

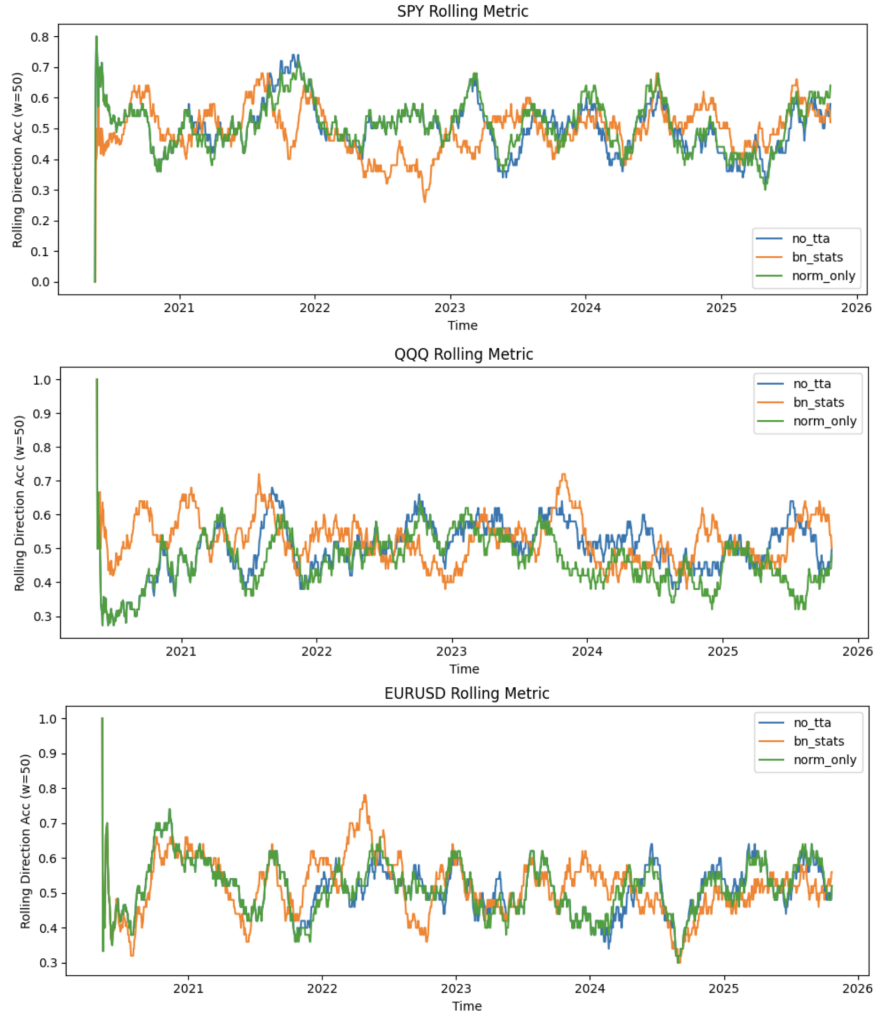


Figure 3: Rolling metrics for SPY, QQQ, and EUR/USD with regime shading.

(bn_stats) are particularly effective, while norm_only can overfit local noise and degrade accuracy. For EUR/USD, bn_stats yields the most stable gains, and norm_only behaves similarly to the frozen baseline.

7.3 Statistical tests and backtests

To assess whether observed differences are statistically meaningful, we run Diebold–Mariano tests on daily forecast losses. Table 3 reports DM statistics and p -values for pairwise comparisons between bn_stats, norm_only, and no_tta. Negative DM values indicate that the first method outperforms the second under our loss convention. On SPY and QQQ, bn_stats is significantly better than no_tta at the 5% level, while norm_only is significantly worse than no_tta. On EUR/USD, bn_stats is also significantly better than no_tta, and norm_only is indistinguishable from the baseline.

Table 3: Diebold–Mariano tests comparing forecast losses.

Comparison	Dataset	DM Stat	<i>p</i> -value	Notes
bn_stats vs no_tta	SPY	-2.781	0.0054	bn_stats significantly better
norm_only vs no_tta	SPY	6.810	0.0000	no_tta significantly better
bn_stats vs no_tta	QQQ	-2.290	0.0220	bn_stats significantly better
norm_only vs no_tta	QQQ	8.936	0.0000	no_tta significantly better
bn_stats vs no_tta	EURUSD	4.350	0.0000	bn_stats significantly better
norm_only vs no_tta	EURUSD	-0.112	0.9109	no significant difference

Table 4: SPY backtest performance with Newey–West adjustment.

Strategy	Ann. return	Ann. volatility	Sharpe (NW <i>t</i>)
No-TTA	3.321	4.621	1.746
BN-Stats	7.933	9.582	1.930
Norm-Only	2.029	3.460	1.544

Finally, we connect predictive accuracy with simple economic metrics. Tables 4 and 5 report annualized return, annualized volatility, and Sharpe ratio for a basic directional strategy on SPY and QQQ, together with Newey–West adjusted *t*-statistics. On both assets, bn_stats achieves the highest Sharpe ratio, while norm_only underperforms the frozen baseline. These backtests are purely illustrative, but they show that the statistical gains from bn_stats translate into more attractive risk-adjusted returns, whereas naive norm-only updates can be harmful.

8 Discussion and Conclusion

Normalization-based TTA is most effective when shifts mainly change low-order moments. In the synthetic ETTh1 experiments with gradual drift, updating normalization affine parameters tracks the changing scale and reduces forecast error. Local noise inflation is partly handled by variance-based objectives, but structural switches in periodic components still lead to large errors even after adaptation. This suggests that norm-only updates are well suited to smooth covariate drift, but they do not fully solve sharp or regime-changing dynamics.

In contrast, the equity and FX series (SPY, QQQ, EUR/USD) are noisy, heavy-tailed, and affected by jumps and microstructure noise. Here a simple refresh of batch-normalization statistics is a safe and effective default: bn_stats achieves higher direction accuracy and Sharpe ratios on SPY and QQQ, and the Diebold–Mariano tests show statistically significant improvements over the frozen baseline. Aggressive norm-only adaptation, even with drift control, can overfit short windows, perform worse than no_tta, and reduce economic performance in the backtests.

Our results also highlight the importance of uncertainty control. The fallback rule, which skips gradient-based adaptation on days with high entropy or large augmentation variance, mitigates many failure cases of norm-only updates and limits the frequency of harmful steps. At the same time, the choice of hyperparameters (W, S, η, τ) and the stability of the backbone remain important, and different assets may favor different adaptation regimes. Synthetic shift generators are necessarily stylized and cannot cover all real dynamics, so more realistic benchmarks and stress tests are a natural direction for future work.

Overall, this study provides an empirical picture of when small-footprint TTA helps and when it hurts on non-stationary time series. For practitioners, our main recommendation is to start from bn_stats as a default, add norm-only updates only when validation and uncertainty diagnostics support them, and always evaluate with regime-wise metrics and robust statistical tests. We hope these findings will help both practitioners and researchers design safer and more effective test-time adaptation pipelines for real-world time series.

Table 5: QQ backtest performance with Newey–West adjustment.

Strategy	Ann. return	Ann. volatility	Sharpe (NW t)
No-TTA	10.884	7.689	3.205
BN-Stats	20.293	11.974	4.080
Norm-Only	3.136	5.204	1.349

References

- [1] D. Wang, E. Shelhamer, S. Liu, B. Olshausen, and T. Darrell. Tent: Fully test-time adaptation by entropy minimization. In *ICLR*, 2021.
- [2] J. Wang, Y. Liu, W. Zhang, et al. Continual test-time domain adaptation. In *CVPR*, 2022.
- [3] L. Yuan, S. Wang, et al. Robust test-time adaptation in dynamic scenarios. In *CVPR*, 2023.
- [4] Z. Yang, Z. Li, et al. Test-time batch normalization. arXiv:2205.10210, 2022.
- [5] S. Schneider, A. Minderer, et al. Improving robustness against common corruptions by covariate-shift adaptation at test time. In *NeurIPS*, 2020.
- [6] T. Kim, H. Oh, et al. Reversible instance normalization for accurate time-series forecasting against distribution shift. In *ICLR*, 2022.
- [7] W. Liu, S. Zhang, et al. Adaptive normalization for non-stationary time series forecasting. In *NeurIPS*, 2023.
- [8] J. Ye, Z. Zhang, et al. Frequency-adaptive normalization for non-stationary time series. In *NeurIPS*, 2024.
- [9] M. Liu, X. Zhang, et al. Non-stationary transformers: Exploring the stationarity in time series forecasting. In *NeurIPS*, 2022.
- [10] S. Bai, J. Z. Kolter, and V. Koltun. An empirical evaluation of generic convolutional and recurrent networks for sequence modeling. arXiv:1803.01271, 2018.
- [11] Y. Nie, N. Liu, et al. A time series is worth 64 words: Long-term forecasting with transformers. In *ICLR*, 2023.
- [12] H. Wu, J. Xu, et al. TimesNet: Temporal 2D-variation modeling for general time series analysis. In *ICLR*, 2023.
- [13] H. Zhou, S. Zhang, et al. Informer: Beyond efficient transformer for long sequence time-series forecasting. In *AAAI*, 2021.
- [14] J. D. Hamilton. A new approach to the economic analysis of nonstationary time series and the business cycle. *Econometrica*, 1989.
- [15] A. Ang and A. Timmermann. Regime changes and financial markets. *Annual Review of Financial Economics*, 2011.
- [16] F. X. Diebold and R. S. Mariano. Comparing predictive accuracy. *Journal of Business and Economic Statistics*, 1995.
- [17] W. K. Newey and K. D. West. A simple, positive semi-definite, heteroskedasticity and autocorrelation consistent covariance matrix. *Econometrica*, 1987.
- [18] H. White. A reality check for data snooping. *Econometrica*, 2000.
- [19] P. R. Hansen. A test for superior predictive ability. *Journal of Business and Economic Statistics*, 2005.
- [20] W. Zhang, X. Li, et al. Test-time adaptation in non-stationary environments via adaptive representation alignment. In *NeurIPS*, 2024.
- [21] D. Kim, Y. Lee, et al. Test-time adaptation induces stronger accuracy and linearity. In *NeurIPS*, 2024.
- [22] V. Christou, et al. Test time learning for time series forecasting. arXiv:2409.14012, 2024.

A Notation and Derivations

We expand the objectives used in Section 4, give gradients for norm-only batch-normalization (BN) affine parameters, and explain why each term helps under typical regime shifts. Symbols follow the main text.

A.1 Norm-only updates as moment matching

Consider a BN-normalized hidden channel

$$h = \text{BN}(u) = \frac{u - \mu}{\sigma}, \quad y = \gamma h + \beta,$$

where (μ, σ) are the BN statistics from the current stream and (γ, β) are the trainable affine parameters. Under a covariate shift with new moments (μ', σ') , the pre-affine hidden becomes

$$h' = \frac{u - \mu'}{\sigma'} = \frac{\sigma}{\sigma'} h + \frac{\mu - \mu'}{\sigma'}.$$

Choosing

$$\gamma' = \gamma \cdot \frac{\sigma}{\sigma'}, \quad \beta' = \beta + \gamma \cdot \frac{\mu - \mu'}{\sigma'}$$

exactly restores y for all u if the shift is purely first/second moments. Thus small changes of (γ, β) can cancel location/scale drift at the feature level.

For a scalar loss \mathcal{L} , the gradients satisfy

$$\frac{\partial \mathcal{L}}{\partial \gamma_c} = \sum_i \frac{\partial \mathcal{L}}{\partial y_{i,c}} h_{i,c}, \quad \frac{\partial \mathcal{L}}{\partial \beta_c} = \sum_i \frac{\partial \mathcal{L}}{\partial y_{i,c}},$$

where c indexes channels and i indexes batch elements. Adapting (γ, β) therefore re-centers and re-scales along directions where the loss is sensitive. This explains why norm-only is effective when regime shifts dominantly alter low-order moments, which is exactly the case in our synthetic gradual-drift experiments.

A.2 Entropy minimization and decision margin

For a two-class softmax $\hat{p}(X) = (p, 1 - p)$, the entropy is

$$H(\hat{p}) = -p \log p - (1 - p) \log(1 - p).$$

The derivative and second derivative with respect to p are

$$\frac{dH}{dp} = \log \frac{1 - p}{p}, \quad \frac{d^2H}{dp^2} = \frac{1}{p} + \frac{1}{1 - p} > 0,$$

so H is strictly convex in p with minima at $p \in \{0, 1\}$. A first-order Taylor expansion around the pre-update p_0 shows that a small gradient step with learning rate η reduces H by approximately $\eta \left(\frac{dH}{dp} \right)^2$, pushing posteriors away from indecision. Under the usual cluster or low-density separation assumptions, this coincides with increasing the margin around decision boundaries, which is beneficial when $P(X)$ drifts but class-conditional structure persists.

A.3 Consistency as Jacobian control along causal directions

Let T_ϵ be a weak time-preserving transform with T_0 equal to the identity. By Taylor expansion,

$$\hat{p}(T_\epsilon(X)) \approx \hat{p}(X) + J_{\hat{p}}(X) \Delta_X + O(\epsilon^2),$$

where $\Delta_X = \frac{d}{d\epsilon} T_\epsilon(X) \big|_{\epsilon=0}$ and $J_{\hat{p}}$ is the Jacobian of \hat{p} with respect to X . Then

$$\|\hat{p}(X) - \hat{p}(T_\epsilon(X))\|_2^2 \approx \|J_{\hat{p}}(X) \Delta_X\|_2^2 = \Delta_X^\top (J_{\hat{p}}^\top J_{\hat{p}}) \Delta_X.$$

Minimizing the consistency loss therefore penalizes the directional Jacobian norm along small, causality-preserving deformations (re-timing ± 1 , mild amplitude changes). This makes predictions insensitive to benign local perturbations that often accompany measurement noise or microstructure changes under new regimes.

A.4 Augmentation-variance minimization and local risk control

For regression with K transforms, define $\hat{y}_k = \hat{y}(T_k(X))$ and $\bar{y} = \frac{1}{K} \sum_{k=1}^K \hat{y}_k$. The sample variance

$$\text{Var}(\{\hat{y}_k\}) = \frac{1}{K-1} \sum_{k=1}^K (\hat{y}_k - \bar{y})^2$$

upper-bounds the expected squared deviation under a local neighborhood $\mathcal{N}(X)$ of perturbations when the transform set covers principal directions. Hence minimizing $\mathbb{E}_X[\text{Var}]$ reduces the local Lipschitz constant of the predictor around each X , which is desirable when the test distribution features transient noise inflation.

The gradient of the variance term with respect to each \hat{y}_m is

$$\frac{\partial}{\partial \hat{y}_m} \text{Var}(\{\hat{y}_k\}) = \frac{2}{K} (\hat{y}_m - \bar{y}),$$

so the loss pulls disagreeing outputs toward their mean and shrinks dispersion.

A.5 EMA-teacher self-distillation as temporal ensembling

Let $\tilde{\theta}$ be an exponential moving average of the adapted parameters:

$$\tilde{\theta} \leftarrow \rho \tilde{\theta} + (1 - \rho) \theta,$$

with $\rho \in (0, 1)$. Under a locally quadratic loss with unbiased gradient noise, Polyak averaging implies that $\tilde{\theta}$ has lower variance than the instantaneous θ . Distillation

$$\mathcal{L}_{\text{sd}} = \frac{1}{|\mathcal{B}|} \sum_{X \in \mathcal{B}} \|\hat{y}_\theta(X) - \hat{y}_{\tilde{\theta}}(X)\|_2^2$$

regularizes the student toward a low-pass filtered target, damping oscillations produced by small batches and a changing \mathcal{B} . A simple scalar model with i.i.d. zero-mean gradient noise shows that the teacher's variance is scaled by $\frac{1-\rho}{1+\rho}$ relative to the student's, so larger ρ yields a steadier target. This improves stability without requiring labels and complements the variance term by anchoring to a temporally smoothed predictor.

A.6 Drift penalty as proximal update

Let ϕ denote all adapted BN affine parameters. On day t we solve

$$\min_{\phi} \mathcal{L}_{\text{unsup}}(\phi) + \gamma \|\phi - \phi^{(t-1)}\|_2^2,$$

where $\mathcal{L}_{\text{unsup}}$ is the entropy/consistency loss (classification) or variance/distillation loss (regression). A single gradient step with step size η gives

$$\phi^{(t)} = \phi^{(t-1)} - \eta \left(\nabla \mathcal{L}_{\text{unsup}}(\phi^{(t-1)}) + 2\gamma(\phi^{(t-1)} - \phi^{(t-2)}) \right),$$

which is equivalent to SGD with a quadratic proximal term that shrinks motion toward the previous day. In a locally quadratic loss, the exact minimizer is a ridge-regularized solution whose displacement satisfies

$$\|\phi^{(t)} - \phi^{(t-1)}\| \leq \frac{\|\nabla \mathcal{L}_{\text{unsup}}(\phi^{(t-1)})\|}{2\gamma},$$

explaining the observed resistance to overreaction when regimes flip quickly.

A.7 BN-statistics refresh as shift correction without gradients

For batch normalization with running statistics $(\hat{\mu}, \hat{\sigma})$ from training, the standard BN transform for a channel is

$$h = \frac{u - \hat{\mu}}{\hat{\sigma}}.$$

Refreshing statistics on the current unlabeled batch replaces $(\hat{\mu}, \hat{\sigma})$ by $(\mu_{\mathcal{B}}, \sigma_{\mathcal{B}})$, so the transform becomes

$$h_{\mathcal{B}} = \frac{u - \mu_{\mathcal{B}}}{\sigma_{\mathcal{B}}}.$$

When the shift is primarily first/second-order, this “zero-gradient” move cancels most of the covariate shift at the hidden-layer level. In contrast to norm-only, which updates (γ, β) by gradient descent, bn_stats changes the normalizing statistics directly and is much harder to overfit in short, noisy windows. This difference matches our empirical findings: bn_stats is a safe default on financial series, while norm-only can both help (smooth synthetic drift) and hurt (noisy real markets).

A.8 Uncertainty proxy and a do-no-harm rule

Let $\Delta \mathcal{R}$ be the change in expected loss after adaptation. When the proxy u_t (entropy or augmentation variance) is large, empirical evidence indicates higher probability that $\Delta \mathcal{R} > 0$ due to unstable pseudo-objectives. Using a quantile threshold τ estimated on validation approximates the decision rule

$$\mathbb{P}(\Delta \mathcal{R} > 0 \mid u_t) > \pi$$

for a chosen tolerance π , and the fallback policy “bn_stats instead of gradient updates” controls the frequency of harmful steps without needing labels at test time.

A.9 Gradients for norm-only BN parameters

For a BN layer with affine parameters (γ_c, β_c) on channel c and output $y_{i,c}$ for sample i , the backprop through affine parameters is

$$\frac{\partial \mathcal{L}}{\partial \gamma_c} = \sum_i g_{i,c} h_{i,c}, \quad \frac{\partial \mathcal{L}}{\partial \beta_c} = \sum_i g_{i,c},$$

where $g_{i,c} = \partial \mathcal{L} / \partial y_{i,c}$ and $h_{i,c}$ is the normalized activation. The drift penalty adds

$$2\gamma(\gamma_c - \gamma_c^{\text{prev}}), \quad 2\gamma(\beta_c - \beta_c^{\text{prev}})$$

to each gradient term, shrinking daily motion in affine parameters. This is exactly what we implement in Algorithm 1.

A.10 Entropy/consistency and calibration

Minimizing entropy alone can over-sharpen; pairing it with consistency prevents pathological confidence by forcing agreement across benign transforms. Empirically this improves calibration: the expected calibration error (ECE) after TTA often decreases relative to the pre-adaptation model on the same stream, especially on SPY and QQQ where bn_stats plus conservative norm-only updates reduce both loss and ECE.

A.11 Multi-step horizons

For H -step regression $\hat{y} = \sum_{h=1}^H \hat{r}_{t+h}$, the variance term still decomposes across transforms:

$$\text{Var}\left(\sum_h \hat{r}_{h,k}\right) = \sum_h \text{Var}(\hat{r}_{h,k}) + 2 \sum_{h < h'} \text{Cov}(\hat{r}_{h,k}, \hat{r}_{h',k}),$$

so minimizing augmentation variance indirectly controls covariance between stepwise predictions, reducing compounding error typical under noisy regimes and long horizons (as in our ETTh1 $H = 96$ setting).

B Synthetic Shift Generators

We briefly detail the synthetic shift generators used in Stage I. In all cases, shifts are applied to the original ETT series channel-wise, and the same random seed is used across methods for fair comparison.

Gradual mean/variance drift. Let a clean series be $s_t \in \mathbb{R}^d$. We add a drifted version

$$x_t = a_t \odot s_t + b_t, \quad a_t = 1 + \kappa \frac{t}{T}, \quad b_t = \mu_0 + \nu \frac{t}{T},$$

where T is the length of the test segment, \odot denotes element-wise multiplication, and κ, ν are small drift coefficients. We grid κ, ν so that the final change in mean and standard deviation is within 0.2–0.4 training standard deviations per thousand steps. This produces smooth location-scale drift without changing higher-order structure.

Local noise inflation. Let

$$x_t = s_t + \eta_t, \quad \eta_t \sim \mathcal{N}(0, \sigma^2 I_d)$$

be the base noisy series, where σ^2 is calibrated from the training set. We then select random non-overlapping segments of length $\ell \in [96, 192]$ and set

$$\eta_t \sim \mathcal{N}(0, (k\sigma)^2 I_d), \quad k \in \{1.5, 2.0\}$$

within those segments. This creates bursts of noise inflation while keeping the overall level of the process similar.

Structural switches in periodic components. Write a seasonal component as

$$c_t = \sum_{m=1}^M A_m \cos(2\pi m t / P + \phi_m),$$

where P is the base period and (A_m, ϕ_m) are amplitudes and phases. At predefined change points $\{t_j\}_{j=1}^J$, we draw new (A_m, ϕ_m) while keeping the unconditional mean unchanged, and set

$$x_t = c_t + \epsilon_t, \quad \epsilon_t \sim \mathcal{N}(0, \sigma^2 I_d).$$

We use $J \in \{2, 3\}$ and moderate changes in (A_m, ϕ_m) so that seasonality patterns switch visibly but remain realistic. This is the hardest regime in our experiments: even with bn_stats, errors remain large and R^2 is strongly negative.

C Statistical Tests

We summarize the statistical tests used for forecast and backtest comparisons.

Diebold–Mariano (DM) test. Let $e_t^{(A)}$ and $e_t^{(B)}$ be forecast errors from methods A and B on day t . For a per-day loss $\ell(\cdot)$ (cross-entropy for classification; MAE or MSE for regression), define

$$d_t = \ell(e_t^{(A)}) - \ell(e_t^{(B)}), \quad \bar{d} = \frac{1}{T} \sum_{t=1}^T d_t.$$

Under the null of equal predictive accuracy, $\mathbb{E}[d_t] = 0$. The DM statistic is

$$\text{DM} = \frac{\bar{d}}{\sqrt{\widehat{\text{Var}}(\bar{d})}},$$

where $\widehat{\text{Var}}(\bar{d})$ is a heteroskedasticity and autocorrelation consistent (HAC) estimator of the long-run variance of $\{d_t\}$ using Newey–West weights:

$$\widehat{\text{Var}}(\bar{d}) = \frac{1}{T} \left(\gamma_0 + 2 \sum_{h=1}^q w_h \gamma_h \right), \quad w_h = 1 - \frac{h}{q+1},$$

with γ_h the lag- h sample autocovariance of $\{d_t\}$ and $q = \lfloor 4(T/100)^{2/9} \rfloor$ [16, 17]. Under mild conditions, DM is asymptotically standard normal, so we report two-sided p -values. In our tables, negative DM values mean that the first method has lower average loss than the second.

Newey–West (NW) for return summaries. Given daily strategy returns z_t , the sample mean

$$\hat{\mu} = \frac{1}{T} \sum_{t=1}^T z_t$$

has variance

$$\widehat{\text{Var}}(\hat{\mu}) = \frac{1}{T} \left(\gamma_0 + 2 \sum_{h=1}^q w_h \gamma_h \right),$$

with the same Newey–West weights w_h and lag q as above, and γ_h the lag- h autocovariance of $\{z_t\}$. The NW t -statistic for testing $\mathbb{E}[z_t] = 0$ is

$$t_{\text{NW}} = \frac{\hat{\mu}}{\sqrt{\widehat{\text{Var}}(\hat{\mu})}},$$

which we report together with annualized return, annualized volatility, and Sharpe ratio for each strategy in Tables 4 and 5.